Reaction Kinetics

DOI: 10.1002/anie.201203526

Characterizing the Kinetics of Nanoparticle-Catalyzed Reactions by Surface-Enhanced Raman Scattering**

*Virginia Joseph, Christian Engelbrekt, Jingdong Zhang, Ulrich Gernert, Jens Ulstrup, and Janina Kneipp**

Determining the catalytic activity and the reaction kinetics are key issues when new catalysts are developed, characterized, and introduced. Catalysis at the nanoscale employing nanoparticles has great potential because of their new catalytic properties, high surface-to-volume ratios, and high surface reactivity.[1] In principle, reactions at the surface of metal structures can be studied using molecular surface-specific spectroscopic techniques.[2] The most versatile of these is surface-enhanced Raman scattering (SERS), which has been frequently applied in investigations of different types of reactions at electrochemical interfaces in situ[3] to address, for example, the formation of reaction intermediates,[4] the dependence of electroorganic reactions on electrode potential,[5] and electron transfer in protein systems.[6] Herein we demonstrate that SERS can be used to study directly the kinetics of a catalytic reaction in situ. Our approach is novel by allowing the structural characterization of the reactant and product surface species in the reaction as well as investigating rate constants in the same experiment. This was possible by using separate gold and platinum nanoparticles that were simultaneously attached to the same glass surface. Our method is independent of the optical absorption properties of the reaction products and/or the catalysts.

In order to investigate a metal-catalyzed reaction with SERS or other plasmon-supported approaches,[7] bifunctional metal structures are needed that have plasmonic properties and also act as a catalyst.[8] A number of catalytically active composite nanostructures have been reported to enhance the Raman signals of dye molecules,[9] and SERS has been used to monitor the structural evolution of bimetallic catalytically active Au–Pt nanoparticles.[10] However, direct observations of a catalytic process by SERS have been rare as they require bifunctional nanomaterials.[11] Our approach is different from those previously reported based on composite nanostructures with plasmonic (Au) and catalytic (Pt,[11a] or Pd)[11b] properties, as we have used separate gold and platinum nanoparticles that are simultaneously immobilized on a glass surface. Scanning tunneling microscopy (STM) data indicate that owing to the proximity of the platinum and gold nanoparticles, the molecules can interact with the platinum nanoparticles whilst they reside in the local optical fields provided by the localized surface plasmons of the gold nanoparticles. The versatility, stability, and general applicability of the immobilized gold nanoparticles for studying catalytic reactions are demonstrated by the quantification of the reaction products and the determination of the kinetics with different catalysts. The results reported therefore have implications both for basic catalysis research and analytical applications.

Gold nanoparticles 40 nm in diameter and platinum nanoparticles less than 2 nm in diameter were prepared by reported procedures.[12] Mixtures of these gold and platinum nanoparticles were simultaneously immobilized on a glass surface using 3-aminopropyltriethoxysilane. Figure 1 A shows an SEM image of the surface of the mixed-nanoparticle substrate. The gold nanoparticles are uniformly distributed at the nanoscale, leading also to a homogenous SERS enhancement factor at the microscopic scale (Figure 1 B). The enhancement factor of roughly 10^6 is as high as that recently reported by us for surfaces containing only gold nanoparticles.[13] The presence of the platinum nanoparticles does not diminish the SERS enhancement provided by the gold nanostructures. This is different from composite structures consisting of gold and platinum[9a,14] or palladium.[11b] As shown recently, the immobilization of the nanoparticles renders them stable towards changes in analyte type and concentration.[13,15]

We investigated the catalytic activity of the mixed-nanoparticle surfaces using the reduction of *p*-nitrothiophenol (PNTP) to *p*-aminothiophenol (PATP) with sodium borohydride as a model reaction (Scheme 1). The kinetics of the analogous reaction of nitrophenol with sodium borohydride to give aminophenol has been investigated frequently, in particular using UV/Vis absorption.[16] When platinum nanoparticles act as catalysts, the reaction takes place at the nanoparticle surface.[16d,17] The borohydride ions react with the metal, forming a metal hydride. In the following, rate-

[*] V. Joseph, Prof. Dr. J. Kneipp
Humboldt-Universität zu Berlin, Department of Chemistry
Brook-Taylor-Strasse 2, 12489 Berlin (Germany)
and
BAM Federal Institute for Materials Research and Testing
Richard-Willstätter-Strasse 11, 12489 Berlin (Germany)
E-mail: janina.kneipp@chemie.hu-berlin.de
C. Engelbrekt, Prof. Dr. J. Zhang, Prof. Dr. J. Ulstrup
Technical University of Denmark, Department of Chemistry
Kemitorvet 207, 2800 Kgs. Lyngby (Denmark)
Dr. U. Gernert
Technical University Berlin, ZELMI
Strasse des 17. Juni 135, 10623 Berlin (Germany)

[**] We thank Katrin Kneipp (DTU) for interesting discussions and Franziska Emmerling (BAM) for valuable advice. Financial support from the Lundbeck Foundation (Denmark; C.E., J.Z., and J.U.) and the ERC (grant 259432; J.K. and V.J.) is acknowledged .

Supporting information for this article is available on the WWW under http://dx.doi.org/10.1002/anie.201203526.

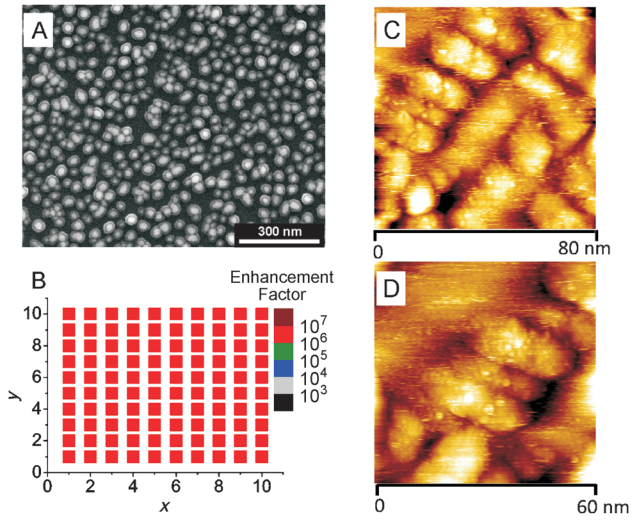

Figure 1. Nanoscopic properties of a substrate with simultaneously immobilized gold and platinum nanoparticles. A) SEM image, scale bar: 300 nm. B) Schematic distribution of enhancement factors at positions (x,y). C, D) STM images of gold and platinum nanoparticles on 80×80 nm^2 and 60×60 nm^2 HOPG substrates, respectively. The SERS enhancement factors in (B) were determined using 5×10^{-6} M crystal violet as the analyte ($\lambda = 633$ nm, intensity: 2.7×10^3 W cm^{-2}, acquisition time: 1 s). Spectra were acquired at a step size of 10 μm, diameter of the probed spot: 1.5 μm (not to scale in the representation).

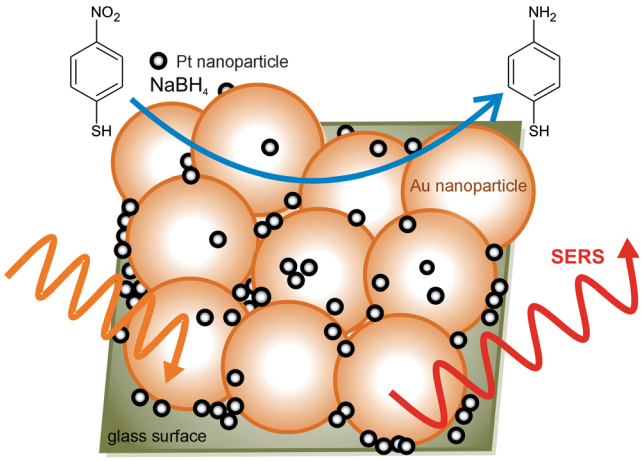

Scheme 1. Representation of the reduction of *p*-nitrothiophenol (PNTP) by sodium borohydride to give *p*-aminothiophenol (PATP), which takes place on mixed-nanoparticle surfaces. The reaction is catalyzed by the platinum nanoparticles, while the surface-enhanced Raman scattering (SERS) signal is brought about by local optical fields of the gold nanoparticles.

limiting step, nitrophenol in contact with the platinum nanoparticle surface is reduced.[16d,17]

In order to achieve detection by SERS, the platinum nanoparticles that interact with the reaction products have to reside in the local optical fields of the gold nanoparticles. Figure 1 C,D display scanning tunneling microscopy (STM) images of the particles on a highly ordered pyrolytic graphite (HOPG) support. Aggregates of gold nanoparticles with smaller spherical features attached are clearly seen; their size fits well with that of the platinum nanoparticles. The platinum nanoparticles are not chemically bound to the gold nanoparticles and can be removed by the STM tip on continuous scanning.

The surfaces were functionalized with 2-naphthalenethiol (2-NT) as the internal standard for relative quantification. 2-NT is not affected by sodium borohydride. Figure 2 A shows the SERS spectra of PNTP, PATP, and 2-NT on immobilized gold nanoparticles.

Figure 2 B shows SERS spectra recorded at selected time intervals after the addition of sodium borohydride to a PNTP/2-NT-functionalized gold/platinum surface. Initially, the spec-

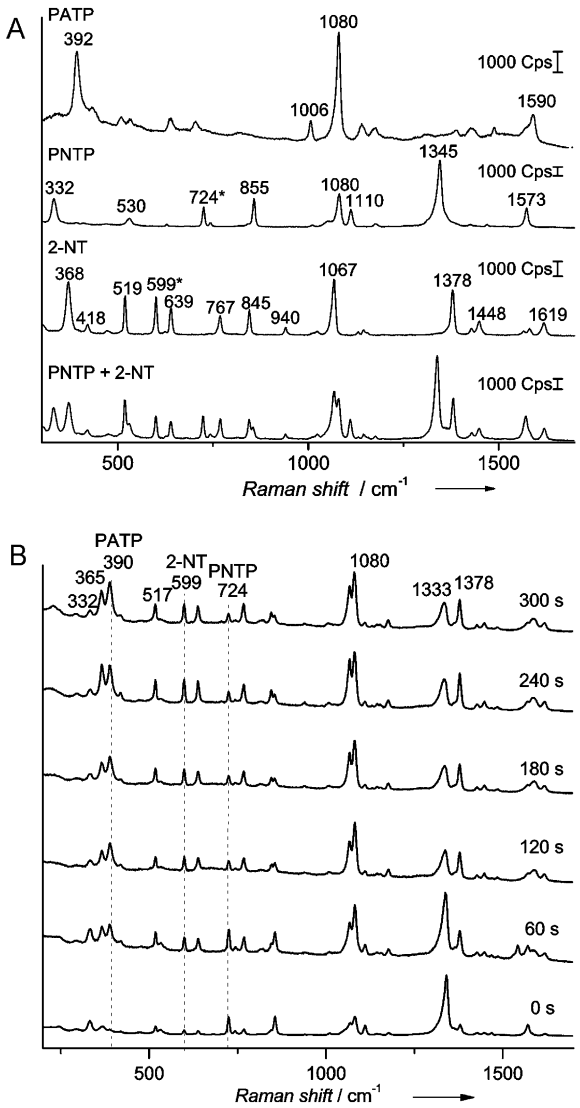

Figure 2. A) SERS spectra of *p*-nitrothiophenol (PNTP), *p*-aminothiophenol (PATP), 2-naphthalenethiol (2-NT), and a mixture of PNTP and 2-NT on APTES-immobilized gold nanoparticles. B) SERS spectra of a substrate with simultaneously immobilized gold and platinum nanoparticles functionalized with a mixture of PNTP and 2-NT at different time intervals after the addition of sodium borohydride ($\lambda = 785$ nm, intensity: 4.8×10^4 W cm^{-2}, acquisition time: 1 s). The spectra are offset vertically for clarity.

trum exhibits bands characteristic of PNTP and 2-NT. After 60 s, the intensity of the PNTP bands decreases significantly and a band at 392 cm^{-1} appears, indicating the formation of PATP (Figure 2B). The spectra provide no evidence of bands that could be assigned to *p*,*p*′-dimercaptoazobenzene (DMAB), which can in principle be generated photochemically from PATP[18] and also from PNTP[19] and which has frequently been found to contribute to the spectra of PATP on silver surfaces.[20] Furthermore, no spectral changes were observed in a control experiment using PNTP-functionalized nanoparticles in the absence of sodium borohydride. We can therefore also exclude the photochemical conversion of PNTP to PATP under our experimental conditions.

To monitor the reaction over time, the intensity of the typical PNTP band at 724 cm^{-1},[21] which is assigned to the C–S stretching vibration, relative to the intensity of the ring deformation band at 599 cm^{-1} of 2-NT[22] was used for quantification. In addition, the appearance of the band at 392 cm^{-1}, which is indicative of the formation of PATP, was monitored. The logarithm of the ratio of the relative intensities at the beginning and at different time points t in the reaction is plotted in Figure 3A. As a large excess of sodium borohydride was used, it can be assumed that the reaction follows pseudo-first-order kinetics.[16] This is similar to the reaction of nitrophenol with catalytic nanoparticles in solution and embedded in sol–gel or polymeric carriers. The reaction rate constant k can be determined by Equation (1).

$$kt = \ln\left(\frac{[PNTP]_{t=0}}{[PNTP]_t}\right) = \ln\left(\frac{(I_{724}/I_{599})_{t=0}}{(I_{724}/I_{599})_t}\right) \quad (1)$$

Here $[PNTP]$ is the concentration of PNTP, and I_{724} and I_{599} are the intensities of the bands at 724 cm^{-1} and 599 cm^{-1}, respectively.

To investigate possible effects of the immobilization of the platinum nanoparticles, we also carried out a modified experiment, in which the surface consisted of only immobilized gold nanoparticles functionalized with PNTP and 2-NT. The platinum nanoparticles and the sodium borohydride were added in solution, in the same ratios to PNTP as in the experiment with immobilized platinum nanoparticles, and the kinetics was monitored by SERS. The result is shown in Figure 3B. The good agreement of the rate constants for the immobilized nanoparticles ($k = 0.011\ s^{-1}$) and for the reaction catalyzed by the nanoparticles in solution ($k = 0.013\ s^{-1}$) suggests that the association of the platinum nanoparticles with the surface has no effect on the reaction kinetics, and that the reaction mechanism is the same in both cases. In contrast to catalytically active nanoparticles embedded in polymer matrices, where diffusion of the reactants is influenced by the properties of the matrix,[23] the nanoparticles immobilized on the surfaces are freely accessible.

The results provide evidence that the immobilized gold nanoparticles can be used to monitor the kinetics of a nanoparticle-catalyzed reaction in solution and hence should be useful to assess the properties of other catalysts as well. Figure 3C shows results for the same reaction in two experiments with the metal acetylacetonates [Cu(acac)$_2$] and [Ni(acac)$_2$] were used as catalysts. Since the relative concentrations of PNTP, 2-NT, and the acetylacetonate catalysts are the same in all experiments, as also confirmed by the band ratio in the SERS spectra (Figure S2 in the Supporting Information), we can compare the properties of the different catalysts. The rate constants of the reactions catalyzed by these transition-metal complexes are smaller than those obtained for the platinum nanoparticles in solution (Figure 3B) and on the surfaces (Figure 3A), giving $k = 0.0036\ s^{-1}$ and $k = 0.0046\ s^{-1}$ for [Ni(acac)$_2$] and [Cu(acac)$_2$], respectively (Figure 3C). The observation that the reaction in the presence of the nickel complex is slightly slower compared than that with the copper complex is in accord with previous work.[24] The reaction is delayed and slowed down in both cases. In particular, a decrease in the signal intensity of PNTP becomes evident only 60 s after the addition of sodium borohydride in the reaction catalyzed by [Cu(acac)$_2$] (Figure 3C). One reason for this delay could be that the active metal hydride complex that has to be present before the

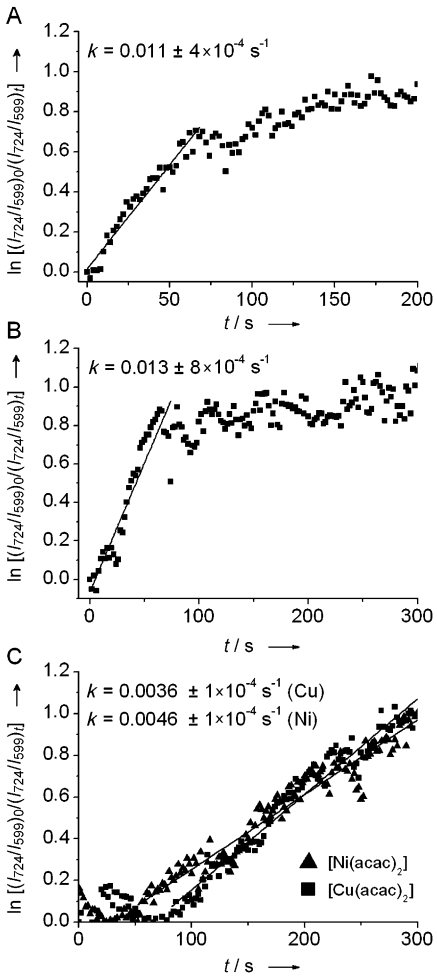

Figure 3. Determination of the rate constants for the reduction of nitrothiophenol with sodium borohydride based on the intensity ratio of the band of PNTP at 724 cm^{-1} and of 2-NT at 599 cm^{-1} in SERS spectra obtained with APTES-immobilized gold nanoparticles. Different catalysts were used: A) platinum nanoparticles immobilized with the gold nanoparticles (see Figure 2B), B) platinum nanoparticles in solution, and C) [Cu(acac)$_2$] (squares) and [Ni(acac)$_2$] (triangles) in solution.

reduction can take place is formed more slowly[24] than the surface complex in the case of the platinum nanoparticles. Another suggestion could be the formation of metal nanoparticles from the metal acetylacetonate in the presence of sodium borohydride,[25] such that these reactions may also be catalyzed essentially by the nanoparticles.

UV/Vis experiments with the same ratio of the catalysts to PNTP and sodium borohydride were conducted for comparison (see the Supporting Information). The relative rate constants obtained with the platinum nanoparticles and metal acetylacetonate complex based on SERS and UV/Vis data, respectively, agree very well (see Figure S1 in the Supporting Information for the UV/Vis data). However, comparison of the absolute rate constants from the SERS and UV/Vis experiments is not possible because of the different experimental conditions. It should be noted that the optical absorption properties of the catalyst and the reaction intermediates can interfere with the detection in kinetic studies based on UV/Vis data. For example, UV/Vis kinetic data with $[Ni(acac)_2]$ as the catalyst cannot be obtained because the absorption of the active metal complex is superimposed on that of PNTP. In contrast, SERS data of the reaction are obtained out of electronic resonance, and are independent of the electronic absorption of the reaction products or the catalyst.

To summarize, we have demonstrated that the kinetics of catalyzed reactions can be followed in situ using surface-enhanced Raman scattering in proximity to aminosilane-immobilized gold nanoparticles. In particular, we have shown that catalytically active Pt nanoparticles can be mixed separately with the plasmonic nanoparticles on the surfaces, thereby generating a nanostructured surface with both plasmonic and catalytic properties. This type of approach has not been reported before. The results indicate that owing to the proximity of the reactants interacting with the catalyst nanoparticles to the gold nanoparticles, the relative quantification of reaction products based on SERS and extraction of kinetic data is possible, independent of the presence of intermediate species. Thus the species in the reaction can be structurally characterized and the rate constants determined in the same experiment.

The application of plasmonic nanoparticle surfaces combines the advantages of easy preparation (composite nanoparticles are not required) and high versatility in terms of the catalyst. This is particularly the case when catalytically active nanoparticles are integrated into a stable mixed-nanoparticle layer, which shows the same high enhancement as a layer containing only plasmonic gold nanoparticles. The approach has further enabled us to compare reaction rate constants of different catalytic systems and the underlying kinetics such as the formation of the active species.

Experimental Section

Gold nanoparticles were synthesized by citrate reduction of tetrachloroauric(III)acid according to Ref. [12a]. Platinum nanoparticles were synthesized following the saccharide-based approach for the synthesis of metallic nanostructures (the SAMENS method) in phosphate buffer (pH 9) according to Ref. [12b]. Gold and mixed platinum/gold nanostructured surfaces were prepared by immobilization of nanoparticles (particle ratio 1:1 in the mixture) by 3-aminopropyltriethoxysilane.[26]

Raman experiments were performed using a Raman microscope while the catalytic reaction was running (for details see the Supporting Information). SERS enhancement was estimated as described in Ref. [27] Scanning electron microscopy images were obtained using a Hitachi S-4000 with a cold field emitter. The acceleration voltage was 15 kV. STM measurements were carried out using a Molecular Imaging (Agilent, USA) instrument with a tungsten tip (Ø 0.25 mm). The tip was sharpened by electrochemical etching of a tungsten wire in 1M KOH.

Received: May 7, 2012
Published online: ■■ ■■, ■■■■

Keywords: gold nanoparticles · heterogeneous catalysis · platinum nanoparticles · surface-enhanced Raman scattering (SERS)

[1] a) B. Hammer, J. K. Norskov, *Impact of Surface Science on Catalysis*, *Vol. 45*, (*Adv. Catal.*, *Vol. 45*), **2000**, pp. 71–129; b) P. S. Jensen, Q. Chi, J. Zhang, J. Ulstrup, *J. Phys. Chem. C* **2009**, *113*, 13993–14000; c) R. Narayanan, M. A. El-Sayed, *Nano Lett.* **2004**, *4*, 1343–1348.

[2] a) M. Arenz, K. J. J. Mayrhofer, V. Stamenkovic, B. B. Blizanac, T. Tomoyuki, P. N. Ross, N. M. Markovic, *J. Am. Chem. Soc.* **2005**, *127*, 6819–6829; b) P. Cremer, C. Stanners, J. W. Niemantsverdriet, Y. R. Shen, G. Somorjai, *Surf. Sci.* **1995**, *328*, 111–118; c) S. Lehwald, H. Ibach, J. E. Demuth, *Surf. Sci.* **1978**, *78*, 577–590.

[3] a) J. Kim, A. A. Gewirth, *J. Phys. Chem. B* **2006**, *110*, 2565–2571; b) Z.-Q. Tian, B. Ren, *Annu. Rev. Phys. Chem.* **2004**, *55*, 197–229.

[4] a) N. F. L. Machado, C. Ruano, J. L. Castro, M. P. M. Marques, J. C. Otero, *Phys. Chem. Chem. Phys.* **2011**, *13*, 1012–1018; b) R. J. Taylor, Y. X. Jiang, N. V. Rees, G. A. Attard, E. L. Jeffery, D. J. Willock, *J. Phys. Chem. C* **2011**, *115*, 21363–21372.

[5] a) P. Gao, D. Gosztola, M. J. Weaver, *J. Phys. Chem.* **1988**, *92*, 7122–7130; b) Y. Zhang, M. J. Weaver, *Langmuir* **1993**, *9*, 1397–1403.

[6] H. Wackerbarth, U. Klar, W. Gunther, P. Hildebrandt, *Appl. Spectrosc.* **1999**, *53*, 283–291.

[7] D. Seo, G. Park, H. Song, *J. Am. Chem. Soc.* **2012**, *134*, 1221–1227.

[8] X. J. Gu, K. L. Akers, M. Moskovits, *J. Phys. Chem.* **1992**, *96*, 383–387.

[9] a) N. T. Flynn, A. A. Gewirth, *J. Raman Spectrosc.* **2002**, *33*, 243–251; b) H. Liu, Q. Yang, *J. Mater. Chem.* **2011**, *21*, 11961–11967; c) L. Lu, G. Sun, H. Zhang, H. Wang, S. Xi, J. Hu, Z. Tian, R. Chen, *J. Mater. Chem.* **2004**, *14*, 1005–1009.

[10] a) L. Guerrini, E. Lopez-Tobar, J. V. Garcia-Ramos, C. Domingo, S. Sanchez-Cortes, *Chem. Commun.* **2011**, *47*, 3174–3176; b) Z.-Q. Tian, B. Ren, J.-F. Li, Z.-L. Yang, *Chem. Commun.* **2007**, 3514–3534.

[11] a) W. Xie, C. Herrmann, K. Koempe, M. Haase, S. Schluecker, *J. Am. Chem. Soc.* **2011**, *133*, 19302–19305; b) K. N. Heck, B. G. Janesko, G. E. Scuseria, N. J. Halas, M. S. Wong, *J. Am. Chem. Soc.* **2008**, *130*, 16592–16600.

[12] a) P. C. Lee, D. Meisel, *J. Phys. Chem.* **1982**, *86*, 3391–3395; b) C. Engelbrekt, K. H. Sørensen, T. Lübcke, J. Zhang, Q. Li, C. Pan, N. J. Bjerrum, J. Ulstrup, *ChemPhysChem* **2010**, *11*, 2844–2853.

[13] V. Joseph, M. Gensler, S. Seifert, U. Gernert, J. P. Rabe, J. Kneipp, *J. Phys. Chem. C* **2012**, *116*, 6859–6865.

[14] Z.-Q. Tian, Z.-L. Yang, B. Ren, J.-F. Li, Y. Zhang, X.-F. Lin, J.-W. Hu, D.-Y. Wu, *Faraday Discuss.* **2006**, *132*, 159 – 170.
[15] L. Chen, X. Han, J. Yang, J. Zhou, W. Song, B. Zhao, W. Xu, Y. Ozaki, *J. Colloid Interface Sci.* **2011**, *360*, 482 – 487.
[16] a) S. K. Ghosh, M. Mandal, S. Kundu, S. Nath, T. Pal, *Appl. Catal. A* **2004**, *268*, 61 – 66; b) Y. Khalavka, J. Becker, C. Sönnichsen, *J. Am. Chem. Soc.* **2009**, *131*, 1871 – 1875; c) N. Pradhan, A. Pal, T. Pal, *Colloids Surf. A* **2002**, *196*, 247 – 257; d) S. Wunder, F. Polzer, Y. Lu, Y. Mei, M. Ballauff, *J. Phys. Chem. C* **2010**, *114*, 8814 – 8820.
[17] S. Saha, A. Pal, S. Kundu, S. Basu, T. Pal, *Langmuir* **2010**, *26*, 2885 – 2893.
[18] a) Y.-F. Huang, H.-P. Zhu, G.-K. Liu, D.-Y. Wu, B. Ren, Z.-Q. Tian, *J. Am. Chem. Soc.* **2010**, *132*, 9244 – 9246; b) B. Dong, Y. Fang, X. Chen, H. Xu, M. Sun, *Langmuir* **2011**, *27*, 10677 – 10682.
[19] B. Dong, Y. Fang, L. Xia, H. Xu, M. Sun, *J. Raman Spectrosc.* **2011**, *42*, 1205 – 1206.
[20] a) N. Matsuda, T. Sawaguchi, M. Osawa, I. Uchida, *Chem. Lett.* **1995**, *24*, 145 – 146; b) N. Matsuda, K. Yoshii, K. Ataka, M. Osawa, T. Matsue, I. Uchida, *Chem. Lett.* **1992**, 1385 – 1388.
[21] B. O. Skadtchenko, R. Aroca, *Spectrochim. Acta Part A* **2001**, *57*, 1009 – 1016.
[22] R. A. Alvarez-Puebla, D. S. Dos Santos, R. F. Aroca, *Analyst* **2004**, *129*, 1251 – 1256.
[23] a) M. A. Mahmoud, B. Snyder, M. A. El-Sayed, *J. Phys. Chem. Lett.* **2010**, *1*, 28 – 31; b) Y. Mei, Y. Lu, F. Polzer, M. Ballauff, M. Drechsler, *Chem. Mater.* **2007**, *19*, 1062 – 1069.
[24] K. Hanaya, T. Muramatsu, H. Kudo, Y. L. Chow, *J. Chem. Soc. Perkin Trans. 1* **1979**, 2409 – 2410.
[25] Ö. Metin, S. Özkar, *Int. J. Hydrogen Energy* **2007**, *32*, 1707 – 1715.
[26] G. Chumanov, K. Sokolov, B. W. Gregory, T. M. Cotton, *J. Phys. Chem.* **1995**, *99*, 9466 – 9471.
[27] V. Joseph, A. Matschulat, J. Polte, S. Rolf, F. Emmerling, J. Kneipp, *J. Raman Spectrosc.* **2011**, *42*, 1736 – 1742.

